

Rafał LEONARCIK  
Miroslaw URBANIAK  
Ryszard DĘBKOWSKI

## METHOD FOR ASSESSING THE GRINDING WHEELS OPERATIONAL PROPERTIES

### METODA OCENY WŁAŚCIWOŚCI EKSPLOATACYJNYCH ŚCIERNIC\*

*The paper presents a new, multi-criteria method which allows the numerical evaluation of the machining process in terms of efficiency, quality and costs. Three indicators were developed to assess the operational properties of grinding wheels. Their values are determined on the basis of the results of short grinding tests carried out on a special test stand. The evaluation of the proposed indicators is described. Furthermore, the application example of this method in determining the grinding wheel's operational properties is presented. In the research, the vitrified alumina oxide grinding wheels were used for grinding of constructional and tool steels of various hardness. The results of the experiments show that the proposed indicators are an effective tool for assessing the process and results of grinding for a specific grinding wheel and material within certain tested grinding parameters range. The study also showed that the differences in indicators' values, observed during tests of grinding specific material type using grinding wheels with different properties, are useful for optimizing the choice of tool type and machining conditions.*

**Keywords:** grinding, grinding wheel, operational properties, grinding wheel characteristics.

*W artykule przedstawiono nową, wielokryterialną metodę, w której grupa trzech wskaźników eksploatacyjnych, wyznaczonych na podstawie danych procesowych z krótkotrwałego testu pracy pary ściernica-przedmiot obrabiany przeprowadzonego na specjalnym stanowisku badawczym, pozwala na liczbowe wartościowanie procesu obróbki pod względem wydajności, jakości i kosztów. Przedstawiono wyniki badań ewaluacji zaproponowanych wskaźników oraz badania aplikacyjne metody w zakresie oceny właściwości eksploatacyjnych ściernic podczas szlifowania stali. W badaniach stosowano ceramiczne ściernice elektrokorundowe oraz stalene narzędziowe i konstrukcyjne o różnej twardości. Wyniki doświadczeń wykazały, że zaproponowane formuły wskaźników są skutecznym narzędziem oceny przebiegu i wyników szlifowania dla określonej pary ściernica-materiał w badanym zakresie wartości nastawnych procesu szlifowania. Badania wykazały także, że różnice wartości wskaźników występujące podczas testów szlifowania określonego rodzaju materiału ściernicami o różnej charakterystyce, są przydatne do optymalizacji wyboru rodzaju narzędzia i warunków obróbki.*

**Słowa kluczowe:** szlifowanie, ściernica, właściwości eksploatacyjne, charakterystyka ściernicy.

### 1. Introduction

Grinding is the basic process of finishing hardened objects and made of difficult-to-cut materials, which allows achieving high level of accuracy in terms of shape and dimension, low surface roughness and low tensile stress in the surface layer [1, 15]. The mentioned values of the machined surfaces are important for the durability and reliability of parts operating independently or as components of devices [35]. The compliance of the grinding results with the requirements given to the workpiece in the design phase is determined by the method of designing and performing the grinding operations. When designing the grinding process, many variables should be taken into account regarding the characteristics of the grinding wheel and its operating conditions, i.e. grinding parameters, the method of cooling the treatment zone, the frequency and way of performing the dressing treatment. Each of these factors has a significant impact on the final result of the treatment, because it affects the phenomena occurring in the contact zone of tribological pair, which is created between the grinding wheel and workpiece material. The impact of abrasive grains on a workpiece can be divided into three stages [8, 11]: elastic deformation and friction between tip and the material, material plastic deformation with the formation of flash and internal friction and chip formation. The share of each of the mentioned stages in the chip formation process depends on the properties of the workpiece, grinding

parameters, friction conditions between the abrasive grains and the workpiece and the geometry of the abrasive grains [2, 11, 28]. As a result of the occurring friction, a significant part of the mechanical energy is largely transformed into heat [20, 23] causing a significant increase in the temperature of the surface layer of the object and its structural changes. Among the negative effects of the thermal impact of the grinding process following can be indicated: grinding burn on the surface layer, phase changes of the material, tempering (softening) with the possibility of repeated hardening of the surface layer, unfavourable residual tensile stresses, grinding cracks and reduced fatigue strength [4, 20, 26]. In order to eliminate these negative effects that the heat has on the workpiece and on the surface of the grinding wheel, the proper cooling liquid (CL), the method of its feeding to the treatment zone and the flow rate should be selected [3, 31]. The second element of the tribological pair – grinding wheel – is subject to wear due to various mechanisms, causing changes in the shape and properties of the tool during machining, therefore reducing the efficiency of the grinding operation and worsening of the quality of the workpiece. The main forms of wear of the grinding wheel surface are abrasive wear and chipping. The vertex of abrasive grains become dulled due to abrasive wear caused by friction on the surface of the workpiece, plastic flow resulting from high temperature and pressure as well as due to chemical reactions that occur at the point of contact

(\*) Tekst artykułu w polskiej wersji językowej dostępny w elektronicznym wydaniu kwartalnika na stronie [www.ein.org.pl](http://www.ein.org.pl)

with the workpiece material. The bond bridges binding abrasive grains are also worn away. Crumbling occurring as a result of the cracking or chipping of abrasive particles and binder bridges is a consequence of impact loads, mechanical and thermal fatigue wear [10,19,22,24,27]. These forms of wear do not occur separately, the domination of one of them depends on the grinding conditions, i.e. the characteristics of the grinding wheel (its structure, type and size of abrasive material, hardness, type of binder) and grinding parameters that change the force exerted on grains. Each of these types of wear affects the final machining result. In the case of volume wear resulting from grain and adhesive chipping, there will be shape errors or dimensional deviations in the workpiece [29]. On the other hand, the creation of flat surfaces at the vertex of the grains increases the power and specific energy of grinding, thermal damage and loss of machining accuracy [19]. The assessment of such conditions is carried out most efficiently with optical measuring techniques [5, 18].

The number of active cutting edges on the surface of the grinding wheel has a significant influence on the interplay of the tribological pair of grinding wheel / workpiece. Unfortunately, due to the random distribution of abrasive grains in the grinding wheel and the assumed dressing conditions, the number of active cutting edges is not a constant value for a particular type of grinding wheel [17, 39]. The grinding forces, the surface roughness, the temperature and efficiency of the grinding process depend on the number and uniformity of the distribution of the active cutting edges [30]. Therefore, for a better control over the grinding process, a group of tools with a defined position of abrasive grains is being developed [9, 40].

As the above description shows, the effect of the grinding operation depends on many simultaneously occurring factors affecting the interaction of the workpiece - grinding wheel pair. The correct selection of grinding wheel determines the success of the grinding operation. The properties of the grinding wheel in interaction with grinding parameters and machined material have a decisive influence on the productivity and the achievable quality of the workpiece.

The evaluation of the grinding wheel operational properties can be made based on physical quantities accompanying the grinding process and the quantities describing the machining result [34]. Drawing conclusions based on the value of one quantity is not sufficiently reliable. Hence in literature, among others [16, 25], suggestions of grinding indicators can be found, which use mathematical equations to combine several characteristic quantities, thanks to which one indicator enables multilateral or thematically directed evaluation of the studied process. These indicators take into account the performance, energy and quality aspects of the grinding process and their formulas contain recognized grinding process sizes [11, 12, 14, 21, 33, 38], such as force, power, temperature and grinding performance, grinding wheel wear, vibration amplitude and acoustic emission, as well as grinding results in the form of parameters for assessing the geometric structure of the surface and the heat affected zone.

Examples of indicators based on which one can adjudicate about the course of the grinding process, including the wheel's operational properties, are represented by formulas (1) – (4). The basic grinding ratio (the so-called  $G$ -ratio) is given by the formula (1). Its high value indicates that the adopted grinding wheel characteristics and grinding conditions ensure high relative efficiency of grinding, as a result of which the share of tool costs in the costs of grinding operations is low.

$$G = \frac{V_m}{V_s} \quad (1)$$

where:

$$\begin{aligned} V_m &- \text{material removal [mm}^3\text{]}, \\ V_s &- \text{grinding wheel wear [mm}^3\text{]}. \end{aligned}$$

The indicators  $K_s$  described in formulas (2) [16] and (3) [25] cover a wide range of grinding process values. In the numerator of both formulas there are values that are high when efficiency of the grinding process increases and wear of the grinding wheel lowers. The denominator takes on smaller values when the grinding effect is a smooth surface and the machining requires low energy consumption. When comparing grinding processes using these indicators, the one with higher value is considered to be better.

$$K_s = \frac{Z'_{max} \cdot G \cdot V'_w}{Rz \cdot W_{sp}} \quad (2)$$

$$K_s = \frac{G}{P_s \cdot Ra} \quad (3)$$

where:

$$\begin{aligned} Z'_{max} &- \text{maximum specific material removal rate [mm}^3\text{/(mm} \cdot \text{s)]}, \\ V'_w &- \text{specific material removal [mm}^3\text{/mm]}, \\ Rz, Ra &- \text{roughness parameters of the machined surface [}\mu\text{m]}, \\ W_{sp} &- \text{specific grinding energy } (W_{sp} = P_s/Z'_{max} \text{ [W/mm}^3\text{/(mm}^3\text{/s)]}), \\ P_s &- \text{grinding power [W]}. \end{aligned}$$

The indicator  $Q'_t$  according to the formula (4) [6], used to assess the cutting ability of the active surface of the grinding wheel, is based on the values obtained from tests performed with a special device outside the machining zone. It determines the velocity of the linear decrement of the sample (tester) approached with a constant force to the rotating grinding wheel.

$$Q'_t = \frac{\Delta l}{\Delta t} \quad (4)$$

where:

$$\begin{aligned} \Delta l &- \text{decrement of the tester length [}\mu\text{m]}, \\ \Delta t &- \text{time of grinding the tester [s]}. \end{aligned}$$

A similar principle of measurement was used by the inventors of the  $G_c$  index [7] to evaluate the process of grinding samples made of ceramic materials with diamond abrasive belts. During the test, the sample is approached with a constant, controlled force to the abrasive belt on a special test device. The material removal rate  $Z_w$  of the grinding carried out under these conditions is a function of the normal grinding force  $F_n$ , the speed of the tape  $v_s$ , and the properties of the sample material  $\Phi_c$  and the cutting properties of the tape  $\Phi_d$ . On the basis of the experimental investigations carried out, the authors [7] found that the material removal rate is proportional to the speed of the tape  $v_s$  and the normal grinding force  $F_n$ . Thus, they assumed that the  $G_c$  index characterizing the interaction of the sample-abrasive tape pair will be defined by the formula (5). Its value, depending on the pair configuration adopted in the tests: the same type of abrasive tape – various sample materials or various abrasive tapes – the same sample material, will depend respectively on the properties of the sample material or the abrasiveness of the abrasive belt.

$$G_c = \frac{Z_w}{v_s F_n} \quad (5)$$

where:

$$\begin{aligned} Z_w &- \text{material removal rate [mm}^3\text{/s]}, \\ v_s &- \text{peripheral speed of the abrasive belt [m/s]}, \\ F_n &- \text{normal force [N]}. \end{aligned}$$

Based on the abovementioned examples, it can be noticed that the number of quantities on the basis of which the value of the index is determined depends on the adopted evaluation criteria and the authors' view on the way of this assessment. However, the inclusion in the indicator of very many values characterizing the grinding process is not favourable due to on their varying variability during the ongoing process. Therefore, it is intended that it contains only quantities that capture the expected grinding effect. And so, if the purpose of grinding is to obtain high quality machining, which is characterized by low roughness of the surface treated and no thermal damage to the surface layer of the workpiece, the indicator should be inversely proportional to the parameters describing these requirements (e.g.  $Ra$  parameter and depth of heat affected zone  $z_T$ ), formula (6) [25]:

$$K_{s1} = f\left(\frac{1}{Ra, z_T}\right) \quad (6)$$

In the case if the goal is high efficiency, the indicator should take into account those process parameters, which will define the volume of the layer being removed per unit of time and those that may accompany this process and at the same time disrupt it. The first should be included in the numerator by increasing the value of the index for an efficient process and the second one in the denominator to reduce the value of the indicator, if the negative phenomena of the assessed process are at a high level. An example of such an indicator is represented by the formula (7), in which it is proposed to apply characteristics such as: maximum specific material removal rate  $Z'_{max}$ , specific material removal  $V'_m$  and vibration amplitude  $x_d$  and degree of wheel loading –  $A_z$  [25]:

$$K_{s2} = f\left(\frac{Z'_{max}, V'_m}{x_d, A_z}\right) \quad (7)$$

Evaluation of the grinding process in the economic terms should mainly take into account the speed of wear of the grinding wheel and energy consumption related to the machining process. The indicator, which accomplishes the above goal (8), contains the grinding ratio  $G$  in the numerator, which refers to the material removal for volume wear of the grinding wheel, and in the denominator of the dimensions that adversely affect the grinding result, but also indicate energy consumption on the machining process, i.e. temperature grinding  $T_{max}$ , components of grinding forces  $F_n$  and  $F_t$ , amplitude of vibrations  $x_d$  and degree of wheel loading  $A_z$  [25]:

$$K_{s3} = \frac{G}{f(T_{max}, F_n, F_t, x_d, A_z)} \quad (8)$$

Despite the use of several measurable quantities in the indicators, no results have yet been obtained that would confirm that it is possible to determine, course and results of the grinding process using one equation. Therefore, in order to obtain transparent information about the examined process, several indicators should be applied, properly selected to the adopted criteria. It also contributes to the lower number of factors that need to be analysed, and thus to easier implementation of the research. Determination of process values, which are inputs to indicators, requires testing with the use of control and measurement equipment which in most cases is only available in research laboratories, not in production conditions. This is a barrier to the precise and efficient design of industrial grinding operations in terms of optimization of the grinding wheel's operational properties.

The above conclusion induced authors to undertake two types of actions. The first was to develop a set of indicators that would charac-

terize the course and results of the grinding process to the widest extent possible, which might also be useful for comparative assessment of grinding wheel's operational properties. The second action was to design the device, useful both in laboratory and industrial conditions, to perform short-term grinding tests, on the basis of which it is possible to determine the values of parameters used in the indicators.

## 2. Description of the method for assessing the wheel's operational properties

In order to evaluate the operational properties in terms of efficiency, quality and economics, a group of three indicators was suggested, that describe the grinding process using the tested grinding wheels.

It has been assumed that the performance indicator  $K_w$  is determined by equation (9):

$$K_w = \frac{Z'}{F'_t} \left[ \frac{mm^3}{N \cdot s} \right] \quad (9)$$

where:

- $Z'$  – specific material removal rate [ $mm^2/s$ ],
- $F'_t$  – tangential grinding force per width unit [ $N/mm$ ].

In the presented equation, the specific material removal rate is related to the tangential component of the grinding force that occurs during machining. This relation determines the amount of material grounded in the time unit per tangential component of the grinding force. A higher value of the indicator means better performance.

The  $K_j$  index, which describes the quality of the surface layer of the workpiece, was determined by the below formula (10):

$$K_j = \frac{F_n}{Ra \cdot F_t \cdot \Delta T_p} \left[ \frac{1}{K \cdot \mu m} \right] \quad (10)$$

where:

- $F_t$  – tangential grinding force [ $N$ ],
- $F_n$  – normal grinding force [ $N$ ],
- $\Delta T_p$  – increase of sample's temperature during the test [ $K$ ],
- $Ra$  – surface roughness of the specimen [ $\mu m$ ].

The quotient of the grinding force components ( $F_n/F_t$ ) used in the index can be treated as the inverse of the tribological contact coefficient combining the removal of the allowance and the friction occurring during the grinding process of the object with the grinding wheel. Its increasing value indicates less smoothing effect of the grinding wheel. The second factor that is important for the quality of the object's surface layer is the heat flow. This was taken into account by introducing an increase in surface temperature  $\Delta T_p$  into the index. What is more, the geometric surface structure of the object was taken into account by introducing the roughness parameter  $Ra$ .

Index  $K_e$  (11), which task is economic description of the machining process, is equal to a well-known G-ratio grinding index expressing the relative grinding efficiency. Its value is the quotient of the material removal  $V_m$  and the grinding wheel wear  $V_s$ :

$$K_e = G \quad (11)$$

Evaluation of the grinding process based on three indicators can give a more complete view on the relations between the grinding wheel and the workpiece, enabling the analysis of grinding wheel abrasive properties in terms of efficiency, quality of the machined surface and the tool's share in the operation costs. The described indicators have

been developed taking into account the possibility of their practical application, paying attention to the scope of the adopted assessment criteria and the ability to easy interpretation of the obtained results.

### 3. Grinding wheel testing device

One of the main design assumptions for the construction of the device was the possibility of its application in industrial conditions and the possibility of its application on various grinders. The designed device, the diagram of which is shown in Figure 1, is adapted to perform tests on surface grinders. The operating principle of device is to transmit cylindrical rotary motion to sample 1 and induce its infeed at constant speed to the active surface of the grinding wheel 9. After contact with a rotating grinding wheel, the plunge grinding of the sample takes place. The applied rotational and radial movement of the sample ensures control over the machining efficiency.

The following can be singled out in the design of the device (fig. 1):

- a belt-driven sample assembly 5 placed on the rolling bearing of double-arm lever 6,
- lever axle 7 mounted directly on the piezoelectric, three-force dynamometer 2,
- pyrometer 8 fixed on the lever perpendicular to the surface of the sample 1,
- actuator 3 with lever thrust screw.

Placing the dynamometer under the lever's axle enabled the evaluation of the grinding forces. The distribution of forces occurring during grinding (Fig. 1) and their projection on the direction of the lever, indicate that the horizontal force component  $P_y$  registered by the dynamometer gets the value of the tangential grinding force  $F_t$ . However, the normal component of the grinding force  $F_n$  can be determined on the basis of equation (12), determined from the conditions of the moment equilibrium referring to the point of application of external force Q (point A in Figure 1):

$$F_n = \frac{P_z \cdot b - F_t \cdot r}{a + b} \quad (12)$$

The described device has been patented [37] and the stand construction, automatic control system and application of the grinding measurement cycle are presented in the article [36]

### 4. Evaluation of indicators of grinding wheels operational properties

In order to assess whether the designed formulas of indicators and the method of obtaining the data necessary to determine them allow obtaining information useful for objective evaluation of wheel performance, tests were performed in various grinding conditions, i.e.:

- grinding with various adjustable parameters on the test device,
- grinding of flat and cylindrical surfaces,
- dry and wet grinding.

The tests were performed on SPG 30x80 (PONAR-Głowno) plane grinders. A sample of cold work tool steel (145Cr6 - 65HRC) was being machined with a vitrified alumina grinding wheel, 1-350x20x127-99A46J7VE01-35. Each test was repeated 3 times due to the grind-

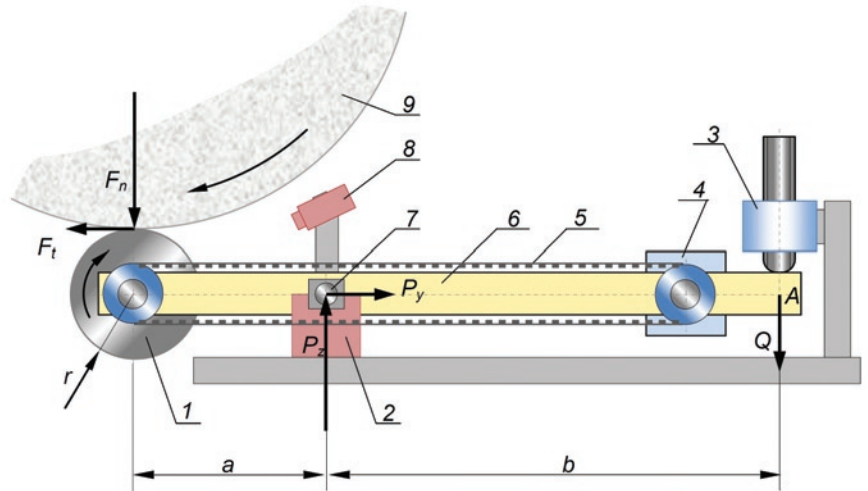


Fig. 1. Diagram of the device testing grinding wheel's operational properties 1 - sample, 2 - dynamometer Kistler type 9317B, 3 - actuator, 4 - sample drive motor, 5 - toothed belt, 6 - lever, 7 - lever axle, 8 - pyrometer, 9 - grinding wheel

ing parameters set out in the test plan. Maintaining the same cutting ability of grinding wheel during testing was ensured by performing a dressing of wheel before each test. For dressing, a single-grain diamond dresser with a specified active diamond width  $b_d$  was used. The dressing feed rate  $f_d$  was selected in order to maintain the same value of the overlap ratio  $k_d = 1,5$  (equation (13)). The dressing infeed  $a_d$  was set at the lever of 0,01mm/pass:

$$k_d = \frac{b_d}{f_d} \quad (13)$$

During the tests, following measurements were made:

- the magnitude of forces loading the dynamometer in the Z and X directions. On the ground of these measurements the components of the grinding forces were determined. The dynamometer load value, resulting from the machining process, was calculated as the difference of the dynamometer measurements, which were recorded in the final part of the test during stable grinding and when there was no contact between the grinding wheel and the object (Fig. 2a),
- increase of the temperature of the sample's surface layer (Fig. 2b),
- wear of the wheel after each test (Fig. 2c),
- sample's roughness (the average of 5 measurements was used for calculations).

Wear of the grinding wheel was assessed basing on a profilogram obtained from a groove shape representation, which was created on the circuit of the grinding wheel as a result of wear processes occurring during grinding of a sample with a smaller width than the grinding wheel. The measurement was carried out with a Hommel-Wave measuring device. An exemplary result of profiling two grinding wheels is shown in Figure 2c.

Studies on the indicators (9) - (11) within the variability range of grinding parameters were carried out on the test device described in p.3 - fig.3.

The tests were performed according to the planned experiment. The sample feed  $a_e$  and the peripheral speed of the  $v_p$  sample were taken as input values. The research was carried out according to the 32-trivalent, two-parameter, full plan, which was generated in the DOE module of the Statistica program. A random option of its layout was chosen to avoid systematic errors in the results of the conducted ex-



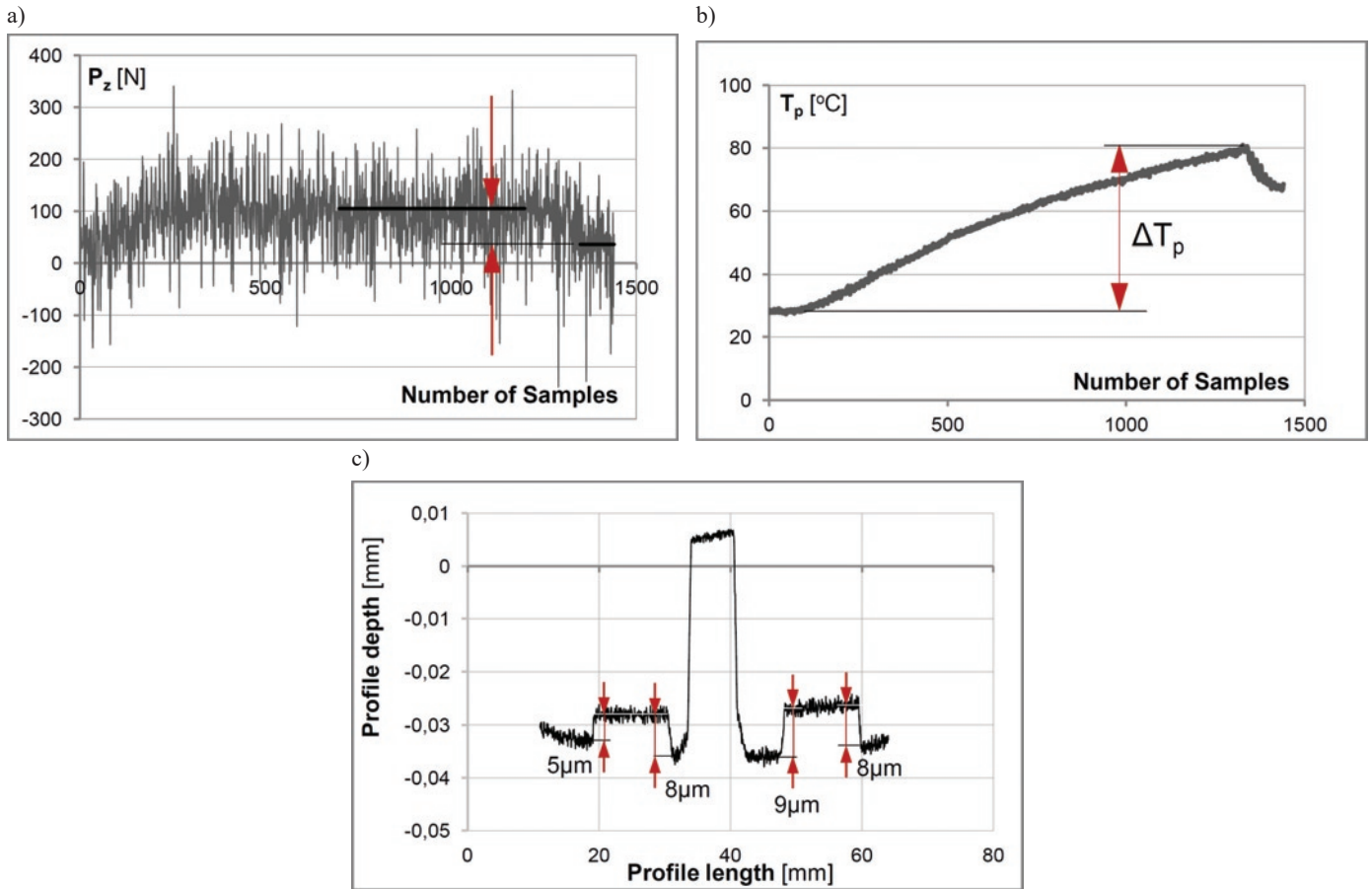


Fig. 2. Measurement results: a) load force of the dynamometer  $P_z$ , b) surface layer temperature of the sample, c) wheel wear

periments. The tests consisted of performing 1-minute trials of plunge grinding of cylindrical samples. The values of grinding parameters used in the tests are summarized in table 1. During the grinding process no cooling liquid was used.

Figure 4 presents graphs and equations of functions approximating the values of  $K_w$ ,  $K_j$ ,  $K_e$  indices which parameters are indeed  $a_e$

Table 1. Values of the test input parameters

Parameter	Value
$a_e$ [mm/rev]	0,005; 0,0125; 0,02
$v_p$ [m/s]	0,15; 0,225; 0,3
$v_s$ [m/s]	26

and velocity  $v_p$ . Approximation of test results was made using power functions, often used in modeling abrasive machining phenomena. These functions accurately reflect the main tendencies in the relations between variable inputs and process results, and are not susceptible to accidental deviations of measured values. The CurveExpert Professional v.1.5 program was used to generate the form of functions and their graphic presentations.

The presented graphs show that the indices calculated according to the proposed formulas react properly to the change of the adjustable parameters of the grinding process.

The value of the specific tangential grinding force included in the grinding efficiency indicator  $K_w$  (9) does not disturb its expected increase after the application of more intensive grinding conditions. This means that for the specific settings of the grinding process, greater values of the indicator will be shown in cases of those pairs of

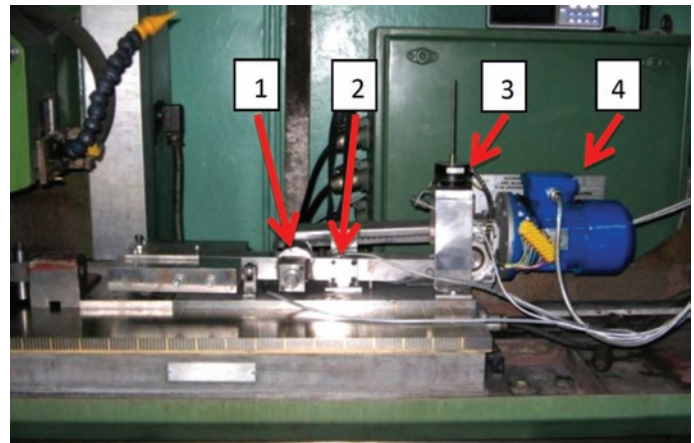


Fig. 3. Device for testing the wheel's operational properties set on the grinder's table SPG 30x80 1 - specimen, 2 - pyrometer, 3 - actuator, 4 - three-phase motor

grinding wheel and material, when the machining allowance is more easily removed.

Similarly, the grinding quality indicator  $K_j$  (10) takes highest values for the most benign machining conditions, that provide the fewest stresses and roughness of the surface layer.

The  $K_e$  (G-ratio) indicator was confirmed to increase its value in the response to more intensive machining with high cutting parameters.

The basis for determining how the indicators behave when using different types of grinding, i.e. when machining cylindrical surfaces and planes, were the results of tests carried out on the specially designed device and directly on the surface grinder, which was equipped

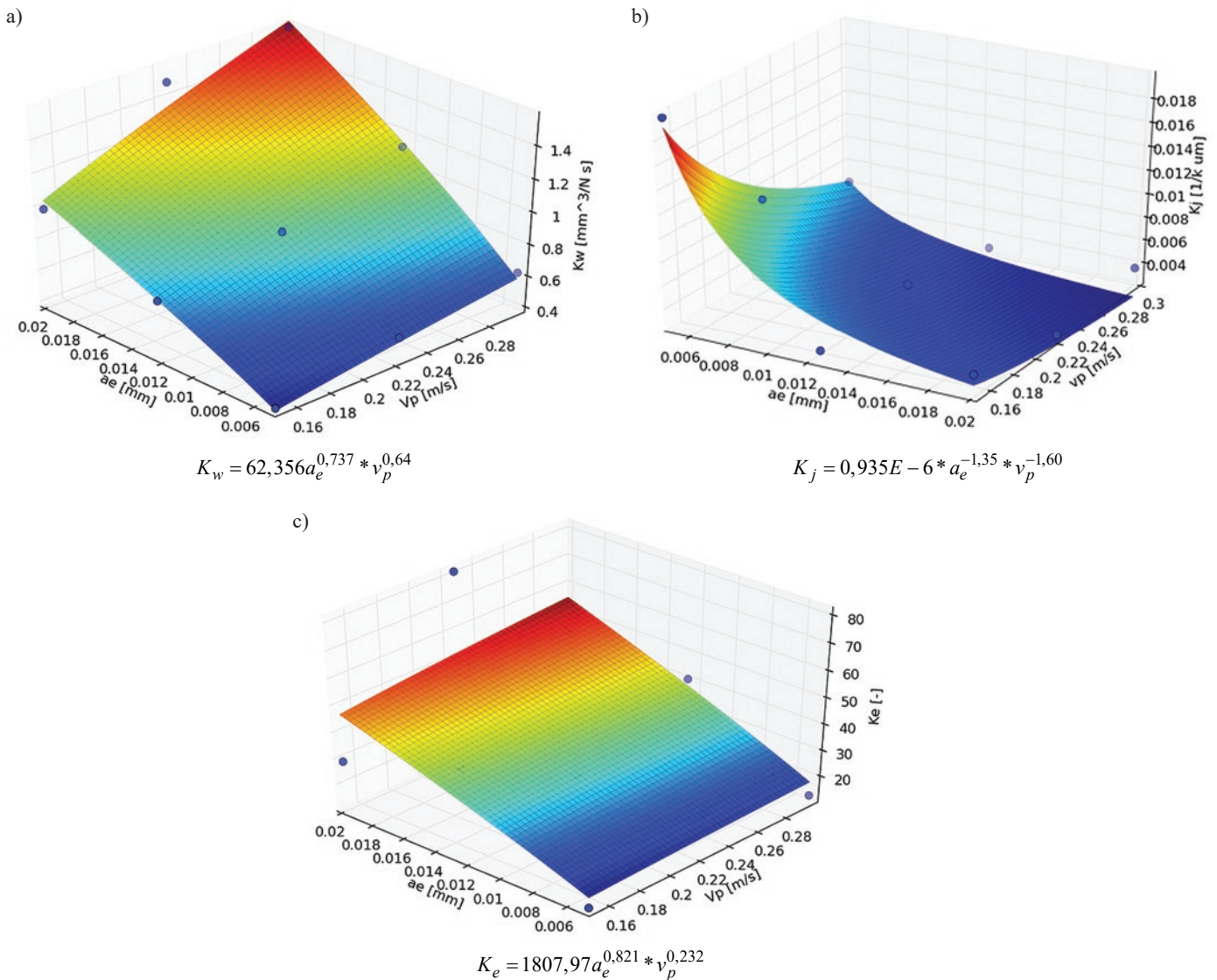


Fig. 4. Relation between the indicators of the wheel operational properties and the grinding parameters (specimen material 145Cr6, grinding wheel 99A46J7VE01)

with a Kistler dynamometer (model 9275) and the same type of pyrometer as in a test device. In both cases, the same values of the adjustable parameters of the grinding process were used (Table 1). In the surface grinding tests cuboidal samples were used with the treated surface's dimensions of 10x250mm. The grinding tests were carried out without the use of a cooling liquid.

Figure 5 presents charts showing the obtained results. The adjustable parameters of the grinding process, i.e.  $a_e$ ,  $v_p$ ,  $v_s$ , were replaced with one  $h_{eq}$  parameter (equivalent chip thickness (14)), which characterizes its intensity:

$$h_{eq} = \frac{a_e \cdot v_p}{v_s} \quad [mm] \quad (14)$$

where:

- $a_e$  – feed rate of the sample [mm],
- $v_p$  – sample's peripheral speed [m/s],
- $v_s$  – grinding wheel peripheral speed [m/s].

The results of the tests show a significant difference in the values of the indices describing the operational properties of the wheel used for surface and cylindrical plunge grinding, (Figure 5). This variety results from different grinding wheel operating conditions in both cases. The heat generated during cylindrical grinding increases the

temperature of the sample much faster, as the grinding wheel remains in constant contact with the machined surface. In the case of surface grinding, when the grinding wheel is outside the machining zone, the heat accumulated by the sample and the grinding wheel is dispersed. However, the bigger contact area of the grinding wheel with the workpiece and the intermittent cutting process during surface grinding, cause more intensive wear of the grinding wheel. The causes are the higher loads that the abrasive grains experience in the chip-forming zone and when hitting of the grinding wheel on the edge of the specimen after reverse.

The above processes have their reflection in the values of the determined indicators. The increase in the temperature of the cylindrical sample in increasingly intensive grinding conditions is not compensated by the lower value of the grinding force, thus the grinding quality index  $K_j$  is getting lower and lower and approaching the value achieved during surface grinding. Surprisingly, there is only a slight increase in the indicator value despite setting the adjustable parameters at their highest values. According to formula (10), in this case it must have had a disproportionately greater increase in the normal grinding force in relation to the other values used in the indicator. It can be assumed that this was a consequence of the inability to machine such chip thickness, which was further the consequence of increased friction and increased wear of the grinding wheel. The economic

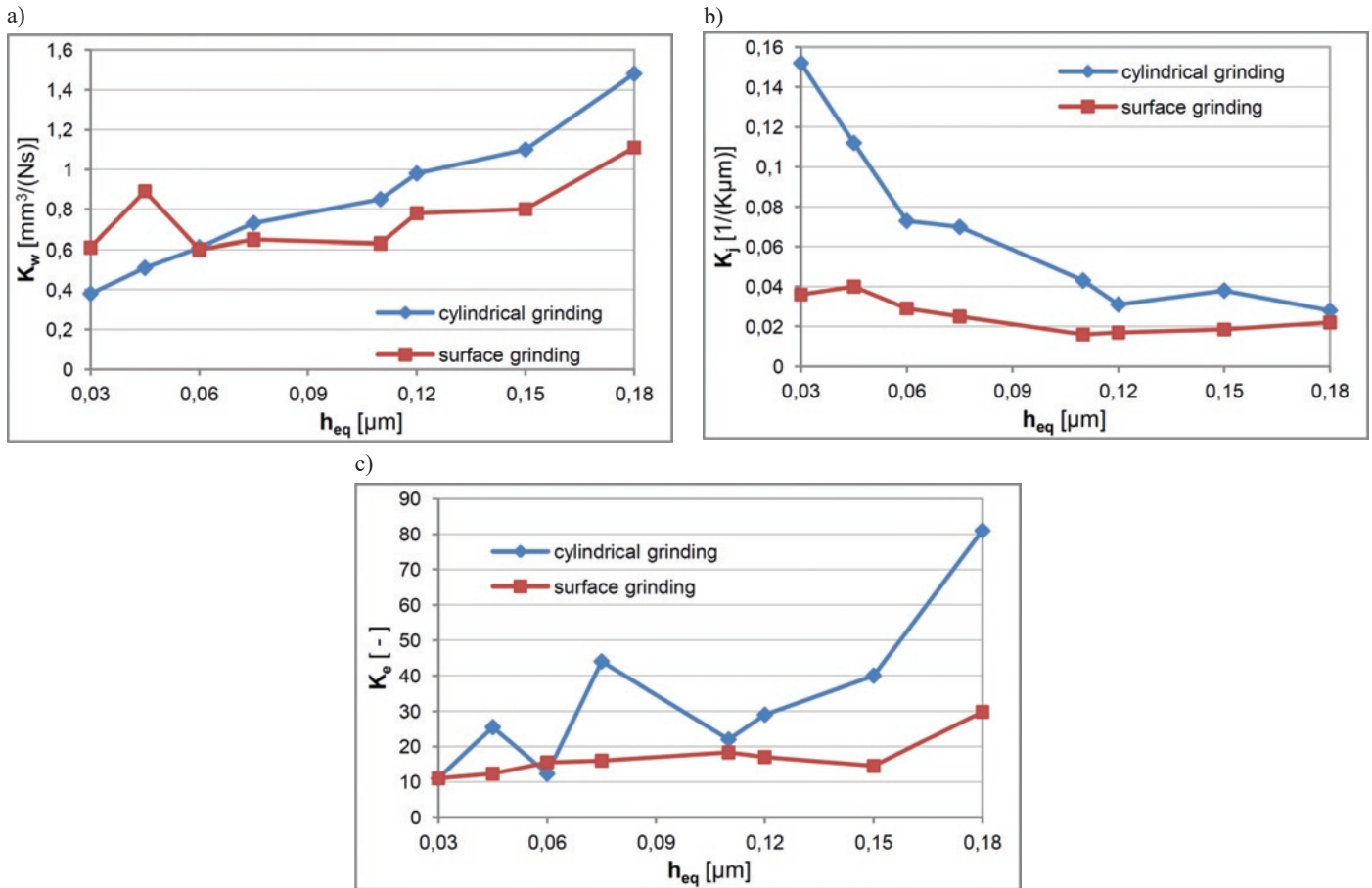


Fig. 5. Relation between the values of grinding wheel's operational indicators  $K_w$ ,  $K_j$  and  $K_e$  and grinding parameters during cylindrical and surface grinding.

efficiency index  $K_e$  confirms this presumption, assuming a lower value for these grinding conditions.

As can be seen, graphs showing the indicators of wheel properties evaluation obtained in cylindrical grinding research are characterised by the greater dynamics of changes. This means that the indicators are characterized by greater sensitivity to changes in the processing conditions and that the proper method of grinding has been used in the developed method.

Tests evaluating indicators in the field of dry grinding and using cooling liquid (CL) were carried out in plane grinding conditions. Due to the inability to perform measurements with the pyrometer during grinding using CL, no qualitative index  $K_j$  was determined, which formula has an  $\Delta T_p$  factor that determines the temperature increase of sample's surface layer. For further analysis, the  $K_w$  and  $K_e$  indexes

were determined and the relation between their values and the grinding adjustable parameters is presented in Figure 6.

Both indicators were of higher, more favourable values in grinding operations carried out without the use of CL due to the grinding wheel operational properties. The use of a cooling liquid reduces the friction between the wheel and the workpiece, making it difficult to the chip formation. Lowering of the friction forces between the cutting edge and the workpiece reduces the tangential stress  $\tau$ , that arises in the chip-forming zone. Thus, in order to form a chip, it is required to increase the depth of cutting edge indentation in the material [15] [32]:

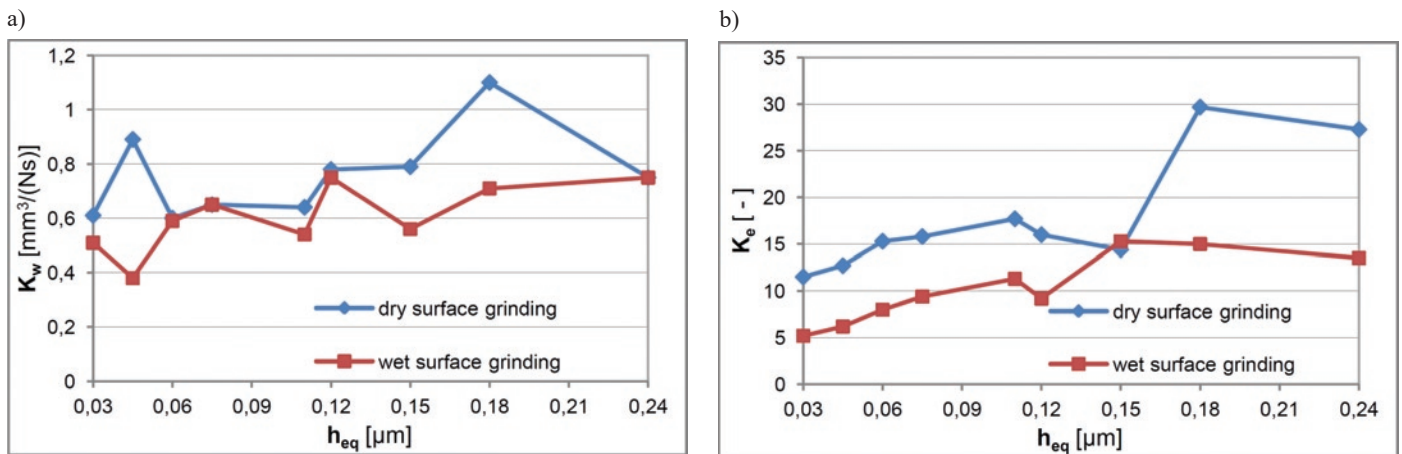


Fig. 6. Relation between the values of grinding wheels' operational indicators  $K_w$  and  $K_e$  and grinding parameters when dry and wet surface grinding



$$h_{\mu} = \rho_k \left\{ 1 - (\cos \eta) \sqrt{0,5 \left( 1 + \frac{\tau}{k} \right)} + (\sin \eta) \sqrt{0,5 \left( 1 - \frac{\tau}{k} \right)} \right\} \quad (15)$$

where:

- $h_{\mu}$  – threshold depth of indentation [ $\mu\text{m}$ ],
- $\rho_k$  – the radius of the sphere described on the abrasive grain [ $\mu\text{m}$ ],
- $\eta$  – cutting angle [ $^{\circ}$ ],
- $k$  – material yield stress during shear [MPa],
- $\tau$  – shear stress [MPa].

Due to the spatial distribution of the cutting edges on the active surface of the grinding wheel, the number of cutting edges that will be able to cut into the required depth decreases. Therefore, efficiency indices  $K_w$  and the tool utilization efficiency  $K_e$  when dry grinding takes on more favorable, higher values. The higher  $K_e$  value when dry grinding also shows that limiting the wear of abrasive by using CL does not compensate for the higher grinding efficiency that is achieved during dry grinding.

The studies discussed above have shown that irrespective of the grinding conditions adopted, the proposed set of indicators and the method of their determination correctly evaluate the course of the grinding process in three aspects relevant to the use and are useful for assessing the wheel performance. Therefore, it should be recognized that the presented indicator formulas are an effective tool for evaluating both the course and results of grinding for a specific grinding / material pair in the tested range of adjustment values in the grinding process, i.e. infeed per revolution of the sample against the grinding wheel  $a_e$  and peripheral speed of the sample  $v_p$ .

## 5. Comparative research on the operational properties of grinding wheels during grinding of steel

The applicability of the discussed method was verified in terms of the choice of grinding wheels for the machining task. The objective of the studies was to check the response of indicators  $K_w$ ,  $K_j$ ,  $K_e$  to changes in the type of grinding wheel used for machining a particular type of material. The course and results of the grinding process carried out with two grinding wheels selected according to the recommendations described in the manufacturer's catalog were evaluated [13]. These are grinding wheels made of friable and monocrystalline alumina with varying grit size, hardness and structure. The tests were carried out for a group of four materials that are normally applied on parts undergoing hardening and grinding.

Table 2 includes the sample materials and characteristics of the recommended grinding wheels. In addition to the grinding wheel characteristics, there is the designation in brackets, which is used later

Table 2. Characteristics of samples and grinding wheels used in the tests

Material	Sample's hardness	Grinding wheel / marking
Alloy cold-work tool steel 100Cr6	55 HRC	1-350x20x127-M463I8VE01NPB5-35 (46I8)
		1-350x20x127-99A46J7VE01-35 (46J7)
Alloy tool steel 145Cr6	65 HRC	1-350x20x127-M463I8VE01NPB5-35 (46I8)
		1-350x20x127-99A46J7VE01-35 (46J7)
Non-alloy quality steel C45	40 HRC	1-350x20x127-99A46L7VE01-35 (46L)
		1-350x20x127-99A60K7VE01-35 (60K)
Alloy special steel 42CrMo4	20 HRC	1-350x20x127-99A46L7VE01-35 (46L)
		1-350x20x127-99A60K7VE01-35 (60K)

in the article. Research was conducted using the same experimental and grinding conditions as in the evaluation of indicators.

### 5.1. Analysis of comparative study results

Figures 7 and 8 show graphs of index values  $K_w$ ,  $K_j$ ,  $K_e$ , which were calculated based on the measured values obtained in the tests. In the charts descriptions grinding wheel characteristics were simplified, giving only their grain, hardness and structure. The title of the graph contains a type of grinding material.

The graphs presented in Figure 7, showing the results of multi-criteria evaluation of two types of grinding wheels used for grinding of steel 145Cr6, indicate that in most of the cutting parameters ranges, the quality of the surface layer of sample  $K_j$  is slightly higher after grinding with a grinding wheel 46J7. Additionally, due to being harder the grinding wheel 46J7 showed a lower relative wear of  $K_e$ . However, the softer grinding wheel 46I8 more easily and efficiently removed the  $K_w$  material, which was probably due to its more intense self-sharpening and a more open structure. The final choice of the grinding wheel and grinding conditions of the 145Cr6 steel can be made by the user, taking into account preferable operational characteristics: the quality provided by the grinding wheel 46J or the efficiency provided by the grinding wheel 46I8.

Grinding tests of the 100Cr6 steel with 46I8 and 46J7 grinding wheels unequivocally indicate the advantage of the 46I8 grinding wheel with the more open structure. Most of the machining parameters of 46I8 are characterized by higher values of grinding indices compared to the grinding wheels 46J7. Only grinding using the lowest infeed and rotational speed of the sample gives an advantage to the grinding wheel 46J7 in terms of the efficiency  $K_w$  and quality of the machining  $K_j$ .

The Figure 8 exemplifies the charts referring to the grinding results of C45 and 42CrMo4 steel using 46L and 60K grinding wheels. Analysis of these graphs indicates that 60K grinding wheel, within the small intervals of parameters values, gives better results compared to C45 steel. Considering more intensive grinding, the 46L grinding wheel gains advantage giving similar surface layer quality  $K_j$  and relatively less wear  $K_e$ . The analysis of grinding process of the 42CrMo4 low hardness steel indicated that the 60K grinding wheel should be recommended and considered as more useful within the whole range of tested grinding parameters. Operational properties indicators of this grinding wheel take lower values compared to the competitive tool only in individual cases.

Summing up, in many cases the indicators of grinding wheels operational properties have similar values, which proves similar usefulness of the tested tools for machining tasks. Differences in indicators value within a specific set of grinding parameters give the possibility of better choice of machining conditions for a particular material.

## 6. Summary

The current challenges standing against production processes, resulting from the growing requirements for product quality, minimizing costs and ensuring the feasibility of implementation, necessitate constant improvement and modernization. Technological operations included in production processes should be transformed towards efficiency and productivity improvement. A way to achieve these goals is multicriteria optimization, which in terms of the grinding process assessment may consist of the grinding wheel operational properties, characterizing the interactions between all process factors. The method presented in the article shows that using short test one can get knowledge about dependencies occurring



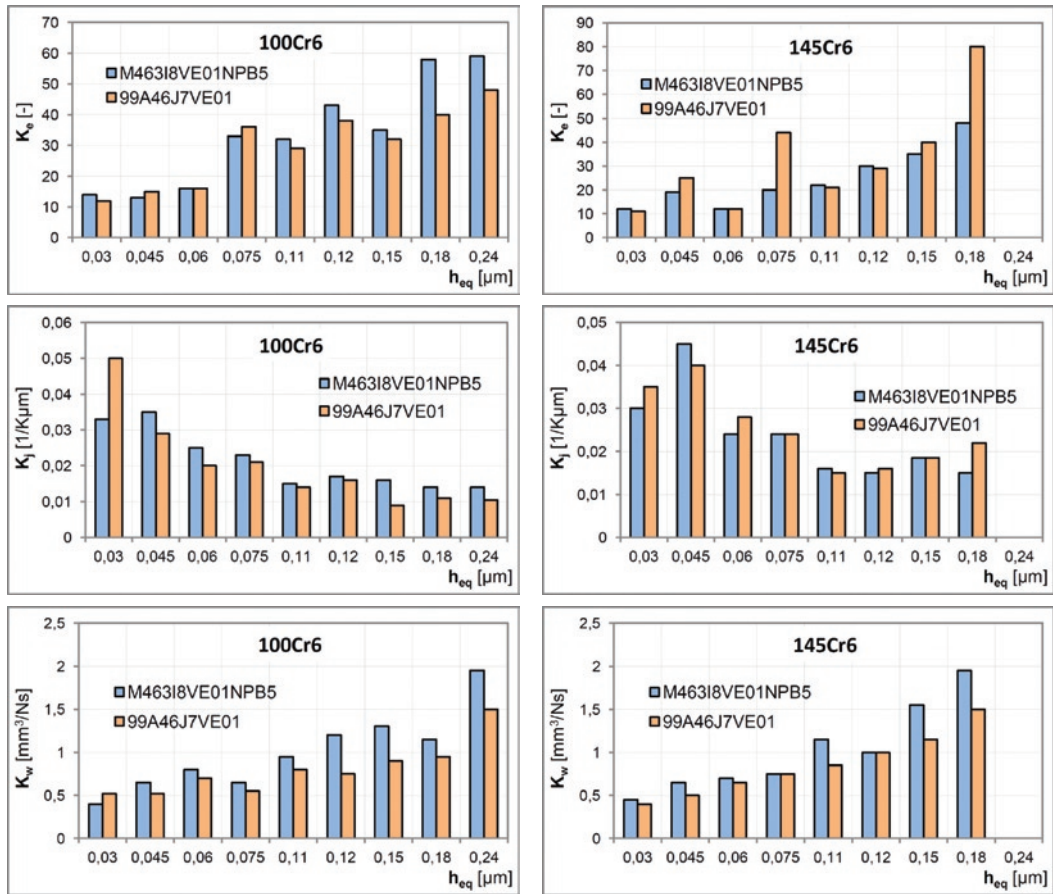


Fig. 7. Operational properties indices for evaluation of M463I8VE01NPB5 and 99A46J7VE01 grinding wheels used for grinding of 100Cr6 and 145Cr6 steels

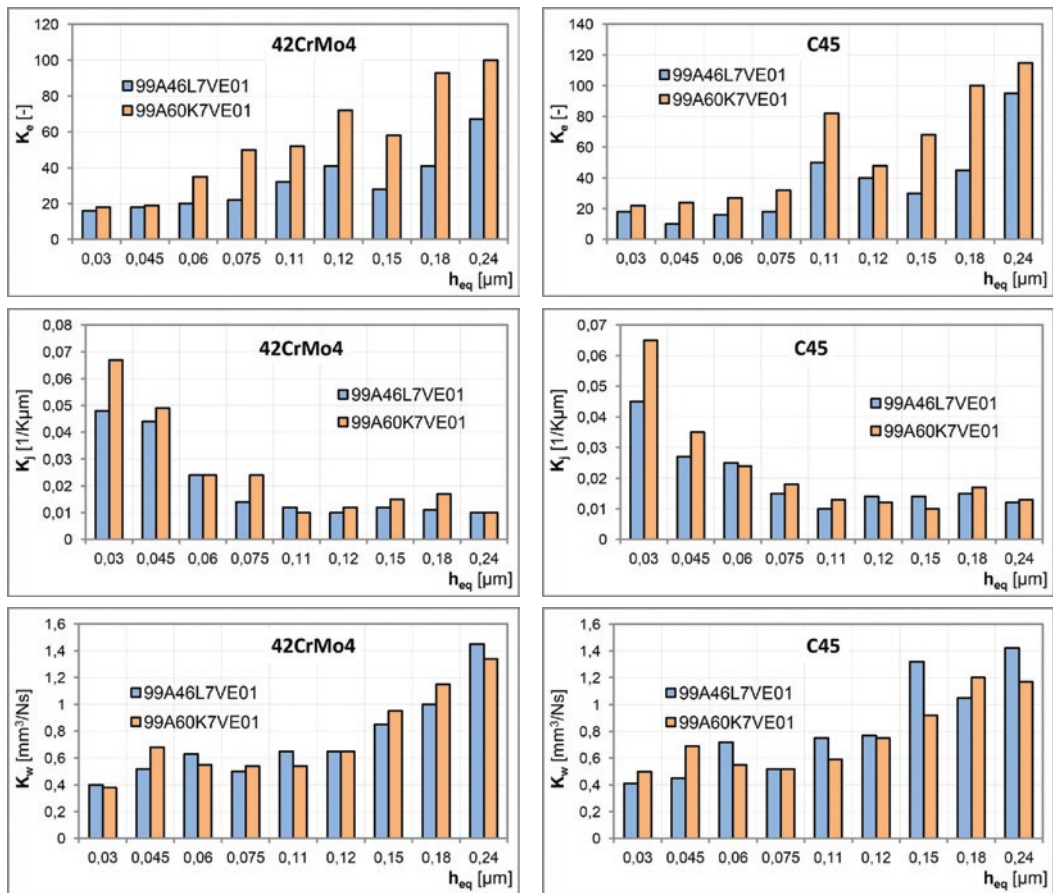


Fig. 8. Operational properties indices for evaluation of 99A46L7VE01 and 99A60K7VE01 grinding wheels used for grinding of 42CrMo4 and C45 steels

in the grinding process, which gives the opportunity to improve at least one of the process characteristics regarding efficiency, costs and quality. The research carried out showed that:

- the range of indicators and formulas adopted correctly characterize the operational properties of grinding wheels, relating them to the process efficiency and cost as well as the quality of the surface layer of the treated surface,
- the grinding variant used in the test device (cylindrical grinding) ensures high sensitivity of the indicators to changes in the grinding conditions, which enables a more unambiguous assessment of the tested grinding wheel's operational properties,

- results of tests on grinding of cylindrical surfaces in dry grinding conditions allow to conclude on the grinding wheel properties in other grinding conditions such as different grinding method or application of cooling liquid.
- due to the varied reaction of the grinding wheel's operational properties to the change of the adjustable parameters of the grinding process, the grinding wheel should be selected based on the values of all presented indicators so that the final decision takes into account the important for the user criteria for the optimized grinding operation.

## References

1. Adibi H, Rezaei Ahmed S M, Sarhan A D. Analytical modeling of grinding wheel loading phenomena. *International Journal of Advanced Manufacturing Technology* 2013; 68: 473-485, <https://doi.org/10.1007/s00170-013-4745-z>.
2. Axinte D, Butler-Smith P, Akgun C, Kolluru K. On the influence of single grit microgeometry on grinding behavior of ductile and brittle materials. *International Journal of Machine Tools and Manufacture* 2013; 74: 12-18, <https://doi.org/10.1016/j.ijmactools.2013.06.002>.
3. Brinksmeier E, Heinzel C, Wittmann M. Friction, Cooling and Lubrication in Grinding *CIRP Annals - Manufacturing Technology* 1999; 48: 581-598.
4. Burakowski T, Wierchoń T. *Surface Engineering of Metals: Principles, Equipment, Technologies*. CRC Press, Boca Raton, 1999.
5. Dębkowski R. Analiza komputerowa obrazu mikroskopowego w zastosowaniu do oceny zużycia czynnej powierzchni ściernicy. *Materiały XXIII Naukowej Szkoły Obróbki Ścierniej*, Rzeszów, 2000.
6. Gołabczak A, Koziarski T. Assessment method of cutting ability of CBN grinding wheels. *International Journal of Machine Tools and Manufacture* 2005; 45: 1256-1260, <https://doi.org/10.1016/j.ijmactools.2005.01.008>.
7. Guo C, Chand R H. Grindability and Mechanical Property of Ceramics. *Proceedings of the 20th Annual Conference on Composites, Advanced Ceramics, Materials, and Structures-A: Ceramic Engineering and Science Proceedings*, 2008: 214-219.
8. Hahn R S. On the mechanics of the grinding process under plunge cut conditions. *Journal of Engineering for Industry* 1966; 1: 72-79, <https://doi.org/10.1115/1.3670895>.
9. Herzenstiel P, Aurich J C. CBN-grinding wheel with a defined grain pattern -extensive numerical and experimental studies, *Machining Science and Technology* 2010; 14: 301-322, <https://doi.org/10.1080/10910344.2010.511574>.
10. Jackson M J, Mills B. Microscale wear of vitrified abrasive materials. *Journal of Materials Science* 2004; 39: 2131-2143, <https://doi.org/10.1023/B:JMSC.0000017776.67999.86>.
11. Kacalak W, Lipiński D, Rypina Ł, Szafraniec F, Tandecka K, Bałasz B. Performance evaluation of the grinding wheel with aggregates of grains in grinding of Ti-6Al-4V titanium alloy. *International Journal of Advanced Manufacturing Technology* 2018; 94: 301-314, <https://doi.org/10.1007/s00170-017-0905-x>.
12. Karpuschewski B, Wehmeier M, Inasaki I. Grinding monitoring system based on power and acoustic emission sensors. *Annals of the CIRP* 2000; 49: 235-240, [https://doi.org/10.1016/S0007-8506\(07\)62936-9](https://doi.org/10.1016/S0007-8506(07)62936-9).
13. Katalog materiałów ściernych. Koło: Andre Abrasives, 2017.
14. Kato T, Fuji H. Temperature measurement of workpieces in conventional surface grinding. *Journal of Manufacturing Science and Engineering* 2000; 122: 297-303, <https://doi.org/10.1115/1.538918>.
15. Klocke F, Brinksmeier E, Weinert K. Capability Profile of Hard Cutting and Grinding Processes. *CIRP Annals* 2005; 54: 22-45, [https://doi.org/10.1016/S0007-8506\(07\)60018-3](https://doi.org/10.1016/S0007-8506(07)60018-3).
16. König W, Messer J. Influence of the Composition and Structure of Steels on Grinding Process. *Annals of the CIRP* 1981; 30: 547-552, [https://doi.org/10.1016/S0007-8506\(07\)60165-6](https://doi.org/10.1016/S0007-8506(07)60165-6).
17. Koziarski A, Golabczak A. The Assessment of the Grinding Wheel Cutting Surface Condition after Dressing with Single Point Diamond Dresser. *International Journal of Machine Tools Design and Research* 1985; 25: 313-325, [https://doi.org/10.1016/0020-7357\(85\)90032-0](https://doi.org/10.1016/0020-7357(85)90032-0).
18. Lipiński D, Kacalak W, Tomkowski R. Methodology of Evaluation of Abrasive Tool Wear with the Use of Laser Scanning Microscopy. *Scanning* 2014; 36: 53-63, <https://doi.org/10.1002/sca.21088>.
19. Malkin S, Cook N H. The wear of grinding wheels. Part 1: attritious wear. *Transactions of ASME, Journal of Engineering for Industry* 1971; 93: 1120-1128, <https://doi.org/10.1115/1.3428051>.
20. Malkin S, Guo C. Thermal analysis in grinding. *CIRP Annals - Manufacturing Technology* 2007; 56: 760-782.
21. Malkin S, Guo C. Thermal analysis of grinding. *Annals of the CIRP* 2007; 56: 760 - 782, <https://doi.org/10.1016/j.cirp.2007.10.005>.
22. Malkin S. The wear of grinding wheels. Part 2: fracture wear. *Transactions of ASME, Journal of Engineering for Industry* 1971; 93: 1129-1133, <https://doi.org/10.1115/1.3428052>.
23. Marinescu I D, Hitchiner M, Uhlmann E, Rowe W B, Inasaki I. *Handbook of Machining with Grinding Wheels*. CRC Press, Boca Raton, 2007.
24. Marinescu I D, Rowe W B, Dimitrov B, Inasaki I. *Tribology of abrasive machining processes*. William Andrew, Inc., Norwich, 2004.
25. Maslov E N.: *Teorija šlifovanja materialov*, Moskva: Mašinostroenie, 1974.
26. Mofdi M, Linghchi M, Zhang T. Applied mechanics in grinding. Part 7: residual stresses induced by the full coupling of mechanical deformation, thermal deformation and phase transformation. *International Journal of Machine Tools and Manufacture* 1999; 39: 1285-1298, [https://doi.org/10.1016/S0890-6955\(98\)00094-7](https://doi.org/10.1016/S0890-6955(98)00094-7).
27. Nadolny K. Wear phenomena of grinding wheels with sol-gel alumina abrasive grains and glass-ceramic vitrified bond during internal cylindrical traverse grinding of 100Cr6 steel. *International Journal of Advanced Manufacturing Technology* 2015; 77: 83-98, <https://doi.org/10.1007/s00170-014-6432-0>.

28. Rasim M, Mattfeld P, Klocke F. Analysis of the grain shape influence on the chip formation in grinding. *Journal of Materials Processing Technology* 2015; 226: 60-68, <https://doi.org/10.1016/j.jmatprotec.2015.06.041>.
29. Rowe W B. *Principles of modern grinding technology*. Elsevier, 2009.
30. Setti D, Ghosh S, Rao P V. A method for prediction of active grits count in surface grinding. *Wear* 2017; 382-383: 71-77, <https://doi.org/10.1016/j.wear.2017.04.012>.
31. Sieniawski J, Nadolny K. The effect upon grinding fluid demand and workpiece quality when an innovative zonal centrifugal provision method is implemented in the surface grinding of steel CrV12. *Journal of Cleaner Production* 2016; 113: 960-972, <https://doi.org/10.1016/j.jclepro.2015.11.017>.
32. Steffens K. Beschreibung eines Gleitlinienfelds für die Deutung der Spanbildung beim Schleifen. *Industrie-Anzeiger* 1979; 19.
33. Stephenson D J. Three Dimensional Finite Element Simulation of Transient Heat Transfer in High Efficiency Deep Grinding. *Annals of the CIRP* 2004; 53: 259-262, [https://doi.org/10.1016/S0007-8506\(07\)60693-3](https://doi.org/10.1016/S0007-8506(07)60693-3).
34. Tönshoff K H, Friemuth T, Becker J C. Process monitoring in grinding. *Annals of the CIRP*, 2002; 51: 551-571, [https://doi.org/10.1016/S0007-8506\(07\)61700-4](https://doi.org/10.1016/S0007-8506(07)61700-4).
35. Uhlmann E, Lypovka P, Hochschild L, Schröer N. Influence of rail grinding process parameters on rail surface roughness and surface layer hardness. *Wear* 2016; 366-367:287-293, <https://doi.org/10.1016/j.wear.2016.03.023>.
36. Urbaniak M, Leonarcik R, Szajder M. *Stanowisko do oceny szlifowalności materiałów*. Naukowa Szkoła Obróbki Ściernej, Gdańsk, 2011.
37. Urbaniak M, Skowron M, Leonarcik R. *Patent nr 213086 na wynalazek pt.: Urządzenie pomiarowe*, 2013.
38. Urbaniak M. *System oceny użytkowych właściwości ściernic*. Łódź: Zeszyty Naukowe P.L., 2002.
39. Wegener K, Hoffmeister W, Karpuschewski B, Kuster F, Hahmann W C, Rabiey M. Conditioning and monitoring of grinding wheels. *CIRP Annals* 2011; 60: 757-777, <https://doi.org/10.1016/j.cirp.2011.05.003>.
40. Yu H, Lu Y, Wang J. Study on wear of the grinding wheel with an abrasive phyllotactic pattern. *Wear* 2016; 358-359: 89-96, <https://doi.org/10.1016/j.wear.2016.04.007>.

---

**Rafał LEONARCIK**

Sonoco Poland - Packaging Services Sp. z o.o.  
Nowy Jozefów 70, 94-406 Łódź, Poland

**Mirosław URBANIAK**

Department of Technology  
Jacob of Paradies University  
Fryderyk Chopin 52 Street, 66-400 Gorzów Wielkopolski,  
Poland

**Ryszard DĘBKOWSKI**

Institute of Machine Tools and Production Engineering  
Lodz University of Technology  
Stefanowskiego 1/15 Street, 90-924 Łódź, Poland

E-mails: rafal.leonarcik@sonoco.com,  
murbaniak@ajp.edu.pl, ryszard.debkowski@p.lodz.pl

---